# Enhanced Luminous Efficacy of White LED with Flat Dual-Layer Remote Phosphor Structure

*Phung Ton THAT*[1], *Nguyen Thi Phuong LOAN*[2], *Nguyen Doan Quoc ANH*[3], *Anh-Tuan LE*[3]

[1]Faculty of Electronics Technology, Industrial University of Ho Chi Minh City,
12 Nguyen Van Bao Street, Ho Chi Minh City, Vietnam
[2]Faculty of Fundamental 2, Posts and Telecommunications Institute of Technology,
11 Nguyen Dinh Chieu Street, Ho Chi Minh City, Vietnam
[3]Faculty of Electrical and Electronics Engineering, Ton Duc Thang University,
19 Nguyen Huu Tho Street, Tan Phong Ward, District 7, Ho Chi Minh City, Vietnam

tonthatphung@iuh.edu.vn, ntploan@ptithcm.edu.vn, nguyendoanquocanh@tdtu.edu.vn,
leanhtuan1@tdtu.edu.vn

DOI: 10.15598/aeee.v18i2.3441

***Abstract.*** *This paper shows the differences in luminous fluxes of two distinguishing dual-layer remote phosphor structures, Flat Dual-Remote Phosphor (FDRP) and Concave Dual-Remote Phosphor (CDRP). The impact of the distance between the two phosphor layers ($d_1$) and the distance from the phosphor layer to the LED surface ($d_2$) on the optical properties of the CDRP is also presented. Specifically, when $d_1$ and $d_2$ are varied, the scattering and absorption characteristics of the remote phosphor layer change dramatically, which enormously influences the color uniformity and illumination capability of WLEDs. The concentration of YAG:$Ce^{3+}$ phosphor also needs to be modified so that the correlated color temperature of WLEDs could be maintained at 8500 K when $d_1$ and $d_2$ are adjusted. In case $d_1 = d_2 = 0$, the scattering and absorption in the remote phosphor layer are minimal, leading to the infinitesimal color and luminous flux. When $d_1$ and $d_2$ get bigger, the scattering surface increases and that the blue and yellow rays are blended becomes more uniform, leading to the minimum white light deviation as well as the lowest luminous flux. According to the studied results, the lumen output can be maximum at 1020 lm if $d_1 = 0.08$ mm or $d_2 = 0.63$ mm while the smallest color deviation occurs when $d_1 = 0.64$ mm or $d_2 = 1.35$ mm. Therefore, the researched results will provide further information for choosing the suitable $d_1$ and $d_2$ in order to improve the quality of WLEDs.*

## Keywords

***Color rendering index, Lambert-Beer law, luminous efficacy, white LED.***

## 1. Introduction

Nowadays, many different light sources are competing in the strongly-growing power market. Solid-state lighting devices such as organic and inorganic light-emitting diodes are indispensable since they are eco-friendly, energy-efficient due to novel "green" technologies. Therefore, requirements for LEDs, such as high efficiencies, energy savings, quick response, and long lifetime, are more advanced [1], [2] and [3]. Although LEDs are getting popular in many fields from displays to general lighting, they still face the challenge of achieving higher luminous flux so that the conversion efficiency and lifetime could be improved, which depends on remote phosphor LEDs inside the phosphor layer separated from the blue-LED chips [4] and [5]. However, matching the phosphor layout with the blue emission pattern of the LED chip is difficult, and this results in a reduction of luminous efficacy. In order to solve these problems, the luminous efficacy should be improved through optimizing the structures or the particle features of the remote phosphor by using patterned or shaped phosphor layers, multi-layer phosphor, nanoparticle-mixed phosphor and new phosphor material [6], [7] and [8]. The second approach is the LED emissions, which need to be mixed by utilizing a lens reflector to accomplish an increase in luminous efficacy.

The concept of chip and layer separation of remote phosphor structures has been analyzed extensively in previous studies [9], [10], [11] and [12]. The enhanced light extraction internal reflection structure, which uses a polymer hemispherical shell lens with an interior phosphor coating, is known to lift up extraction effi-

ciency. Furthermore, if luminous efficiency needs to be enhanced by reflecting downward light, an air-gap embedded structure may be helpful to support it. The concentration of phosphor plays a crucial role in lumen efficacy except for absorption loss in the phosphor layer of the package's structure increasing with the intensification of phosphorus concentration [13], [14] and [15]. Therefore, the lower the Correlated Color Temperature (CCT), the worse the illumination efficiency of the equipment will be [16], [17] and [18]. Several studies have demonstrated that high scattering and reflectance appearances also reduce luminous efficacy [19] and [20]. Hence, enhancing the emission of blue and yellow rays and reducing the amount of light loss from backscattering and reflection are essential.

To achieve higher luminous flux, dual-layer remote phosphor configurations have been proposed in several studies. However, it is difficult for the manufacturer to select an optimum optical structure among various remote phosphor structures. In this study, FDRP and CDRP structures were proposed and validated. Researched results show that the FDRP structure exhibits a significant change in scattering when modifying $d_1$ and $d_2$. When $d_1$ and $d_2$ change, the YAG:$Ce^{3+}$ concentration varies. Therefore, the flux can be controlled via $d_1$ and $d_2$. Unlike the FDRP structure, the scattering of the CDRP structure varies little by modifying the curved radius of the phosphor layer. Consequently, controlling the luminous flux meets some troubles. Moreover, the CDRP structure is difficult to fabricate. This study proposes to use the FDRP structure with a suitable YAG:$Ce^{3+}$ concentration to achieve higher luminous flux.

# 2. Computational Simulation

## 2.1. Phosphor Preparation

The phosphor used in both CDRP and FDRP for the other phosphor layer besides the yellow-emitting YAG:Ce phosphor is $LiLaO_2$:$Eu^{3+}$. $LiLaO_2$:$Eu^{3+}$ is a phosphor that emits red emission color at the highest emission around 1.775–2.02 eV. The raw materials that constitute $LiLaO_2$:$Eu^{3+}$ are $La_2O_3$, $Eu_2O_3$ and $Li_2CO_3$. In this research, $LiLaO_2$:$Eu^{3+}$ phosphor is applied to the packages to create WLEDs with high luminous efficacy and CRI. To generate $LiLaO_2$:$Eu^{3+}$, a 6-step process including mixing ingredients, dehydrating, firing, powderizing, re-firing and re-powderizing, must be strictly followed. First, combine all the ingredients by slurrying them in methanol. Once the combination reaches a homogeneous state, leave them in the air until dry, the dry product then will be ground into powder. In the next step, put the powder in open alumina crucibles and fire at around 600 °C in the condition of air. The outcome is now solidified and needs to be gently powderized before moving onto the next step. In this step, the powder compound is fired again in an open alumina crucibles and airy condition but at 1000 °C for an hour. Similar to the first firing process, the materials are hardened and need a grinding process to become a complete $LiLaO_2$:$Eu^{3+}$ phosphor. The final product should be kept in a well-closed container for preservation and avoiding contamination. Viewers can refer to the detailed chemical composition of this phosphor in Tab. 1.

**Tab. 1:** Chemical composition of red-emitting phosphor $LiLaO_2$:$Eu^{3+}$.

| Ingredient | Mole (%) | By weight (g) |
|---|---|---|
| $La_2O_3$ | 95 (of La) | 155 |
| $Eu_2O_3$ | 5 (of Eu) | 8.8 |
| $Li_2CO_3$ | 101 (of Li) | 37.4 |

## 2.2. Constructing the WLEDs Configuration

It was realized throughout the 3D ray-tracing simulation and LightTools software that the two phosphor films directly affect the optical efficiency of pc-LEDs when the temperature reaches the level of 8500 K. According to the structure of the LED model, a pc-LED is comprised of blue LED chips, two phosphorus layers, one reflector cup, and one silicone layer. We have constructed their precise physical models with the value of normalized cross-correlations approximately 99.6 %, which means the actual packaging and its simulated packaging are alike. Moreover, the impacts of factors such as LED wavelength, waveform, light intensity, and operating temperature on the luminous flux can be reduced.

The simulation of the WLED design used in this study is carried out based on the actual WLED model. The structure of Flat Dual-layer Remote Phosphor configuration (FDRP) and Concave Dual-layer Remote Phosphor configuration (CDRP) have been proposed and compared in light emission performance, as displayed in Fig. 1(a) and Fig. 1(b), respectively. Furthermore, the spectral values of YAG:Ce, including absorption spectrum and emission spectrum, are presented in Fig. 1(c). $d_1$ is defined as the distance between the two layers of phosphor, while the gap of LED surface to the FDRP structure is called $d_2$. Other distances, $r_1$ and $r_2$, are known as the radii of curvature of the upper and lower phosphor layers of the CDRP structure.

A reflector, which is boned with these chips, is 2.07 mm in height and 8 mm in bottom length. In addition, the blue chips that are attached to the reflector is has been designed carefully with precise measurements for the superlative outcomes. Each of them has

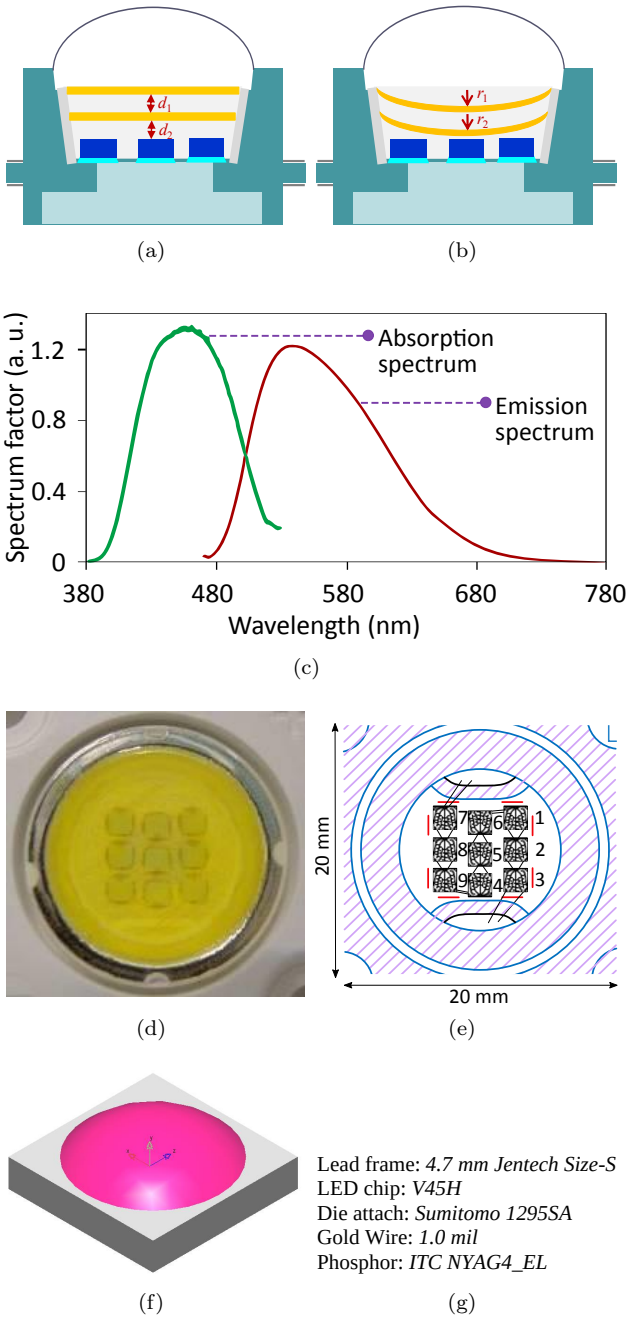


**Fig. 1:** Illustration of FDRP (a), and CDRP (b), (c) the measured spectra of the yellow-emitting YAG:Ce phosphor, (d) the actual WLED packaging, (e) the diagram of chip LED, (f) simulation of WLED packaging, and (g) the parameters of WLED packaging.

a dimension of 1.14 mm × 0.15 mm, the radiant flux of 1.16 W, and the peak wavelength of 453 nm. Moreover, these chips are coated by a phosphor film whose thickness is 0.08 mm, as depicted in Fig. 1. So as to clarify the impacts of using two phosphor layers on the optical performance of LEDs, the process of simulating the optical structure is carried out in accordance with different distances among phosphor layers with the LED. The phosphor particle has a spherical shape with an average diameter of 14.5 μm. The two phosphor films in the WLED simulation are separated, and the distance between them is called $d_1$, while $d_2$ is the gap between the top surface of the chips and the lower phosphor class, as shown in Fig. 1(a). In addition, $d_1$ and $d_2$ are modified during the simulation process for a deeper investigation. Their variation ranges are 0–0.64 mm and 0–1.43 mm, respectively. For the CDRP structure, $r_1$ is a fixed value of 16 mm. The value of $r_2$ is varied between 16.1 mm and 16.9 mm.

When $d_1$ and $d_2$ are adjusted, the lumen output can get the highest level, and the chromatic deviation can be reduced to the lowest value. To keep the color temperature of LED steady at 8500 K, the phosphor concentration needs to be in the range of 14 %–26 % wt. connected with the gap between the phosphor films. In the case of CDRP, the value of $r_1$ is fixed at 16 mm. Meanwhile, the value of $r_2$ is varied between 16 mm and 17 mm. As shown in Fig. 2(c), YAG:$Ce^{3+}$ changes from 16.6 % to 17 % when $r_2$ is changed to keep average CCT. Compared with FDRP as Fig. 2(a) and Fig. 2(b), the change in YAG:$Ce^{3+}$ concentration of the CDRP structure was negligible, so the scattering variation was trivial. It can be predicted that the generated luminous flux does not change significantly in the case of CDRP. In addition, the CDRP structure can be more difficult to fabricate than the FDRP structure. In contrast, the FDRP structure brings about many changes in scattering and absorption in WLEDs. This creates a greater opportunity for controlling output luminous flux.

This model allows us to adjust the phosphor location to find out the optimal distance among phosphor layers that can determine the optical characteristics of LEDs. In the simulation process, the position of the middle phosphor layers is modified; in contrast, that of the top phosphor layer is fixed to the LED chip. Notwithstanding, the placement and arrangement of phosphor layers in a dual-layer package can generate a substantial variation of the correlated color temperature of LEDs due to the absorption, scattering, transmission, and conversion of light. To maintain the same CCT of this package, depending on the distance between two phosphor layers in pc-LEDs, the phosphor concentration needs to be adjusted appropriately, as shown in Fig. 2. Obviously, the phosphor concentration of the dual-layer package has a tendency to drop from 26 % to 14 % in the range of 0–1.43 mm. According to these results, it can be deduced that the phosphor concentration needs to be reduced to ensure that this package's CCT is constant during the simulation process. Another noticeable point is that the concentration of yellow phosphor changes moderately when $d_1$ exceeds 0.08 mm.

Specifically, when $d_1$ climbs from 0 to 0.08 mm, YAG:$Ce^{3+}$ concentration declines sharply from 24.11 % to 16.22 %. Simultaneously, the scattering in the LED

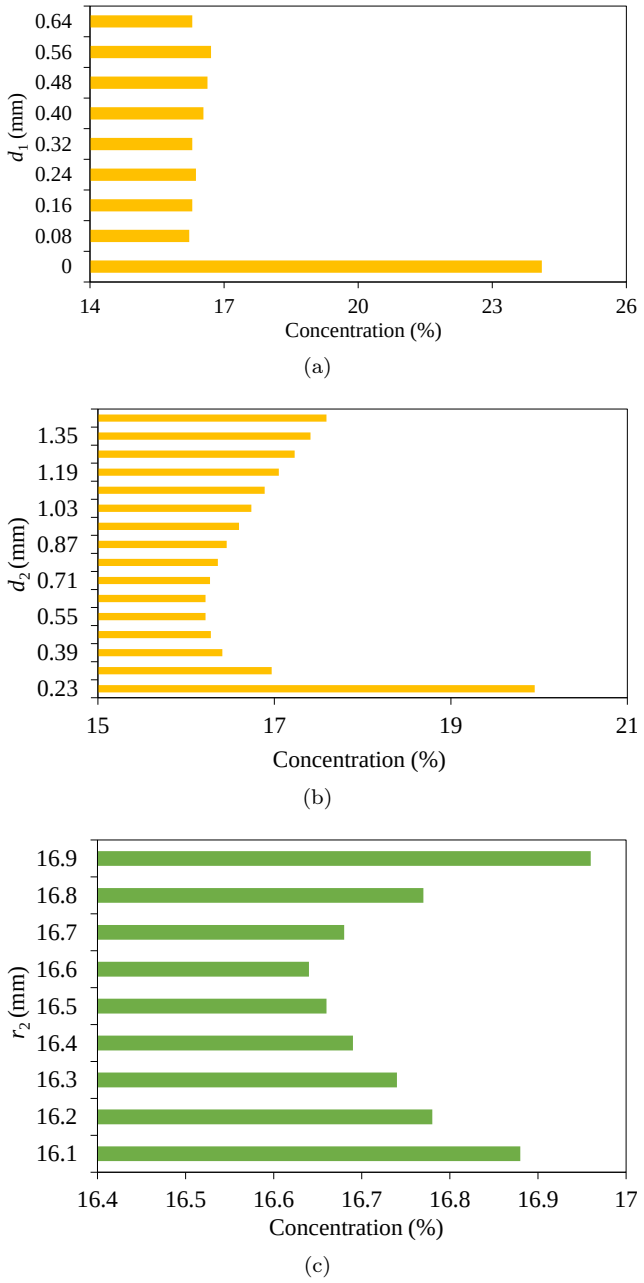


**Fig. 2:** The concentration of yellow phosphor in case of $d_1$ (a), $d_2$ (b) and $r_2$ (c).

packages slumps markedly, which is only conducive to the flux but not to the color uniformity. However, as $d_1$ continues to go up to 0.64, the YAG:$Ce^{3+}$ concentration changes slightly. Similarly, the concentration of YAG:$Ce^{3+}$ falls steeply from 19.55 % to 16.22 % when $d_2$ climbs to 0.55 mm. Then $d_2$ keeps increasing with different YAG:$Ce^{3+}$ concentration. From Fig. 2, it is clear that the distances $d_1$ and $d_2$ have enormous influences on the scattering and absorption of the remote phosphor layer, i.e., which affects the optical properties of the WLEDs.

## 2.3. Computing the Transmission of Light

Presented in this section is the mathematical model for computing the transmitted blue light and converted yellow light in the dual-layer remote phosphor structure. Based on this model, it is possible to achieve a huge enhancement in WLED performance.

The computation for the transmitted blue light and converted yellow light of the structure of single-layer remote phosphor whose phosphor film has a thickness of $2h$ can be presented as [21]:

$$PB_1 = PB_0 \cdot e^{-2\alpha_{B1}h}, \tag{1}$$

$$PY_1 = \frac{1}{2}\frac{\beta_1 \cdot PB_0}{\alpha_{B1} - \alpha_{Y1}}\left(e^{-2\alpha_{Y1}h} - e^{-2\alpha_{B1}h}\right). \tag{2}$$

Meanwhile, the expressions for the transmitted blue light and converted yellow light of dual-layer remote phosphor structure having phosphor layer thickness of $h$ are demonstrated as follows:

$$PB_2 = PB_0 \cdot e^{-2\alpha_{B2}h}, \tag{3}$$

$$PY_2 = \frac{1}{2}\frac{\beta_2 \cdot PB_0}{\alpha_{B2} - \alpha_{Y2}}\left(e^{-2\alpha_{Y2}h} - e^{-2\alpha_{B2}h}\right). \tag{4}$$

Here, $h$ represents the thickness of a phosphor layer in the structures. The subscripts "1" and "2" describe single-layer and dual-layer remote phosphor packages. $\beta$ demonstrates the conversion coefficient for blue light that is converted to yellow light. The blue light intensity (PB) and yellow light intensity (PY) are the intensities of light emitted from the blue LED, presented as $PB_0$. $\alpha$B; $\alpha$Y are parameters describing the fractions of the energy loss of blue and yellow lights in their process of distribution in the phosphor films, respectively.

According to the equation below, the dual-layer remote phosphor model can yield better lighting efficacy for WLEDs than the single-layer one:

$$\frac{(PB_2 + PY_2) - (PB_1 + PY_1)}{PB_1 + PY_1} > 0. \tag{5}$$

To verify the increase of the flux, Fig. 3 depicts the emission spectrum of the dual-layer phosphor. For $d_1$, the emitted spectral intensity when $d_1 = 0$ is smaller than which in the cases $d_1 > 0$ at the two wavelength ranges of 380–480 nm and 480–580 nm. For $d_2$, the blue LED surface is at least 0.23 mm from the lower phosphor layer, resulting in the lowest flux, compared to the case $d_2 > 0.23$ mm. Thus, the photon emitted in the dual-layer phosphor structure is larger than that of the single-layer phosphor structure.

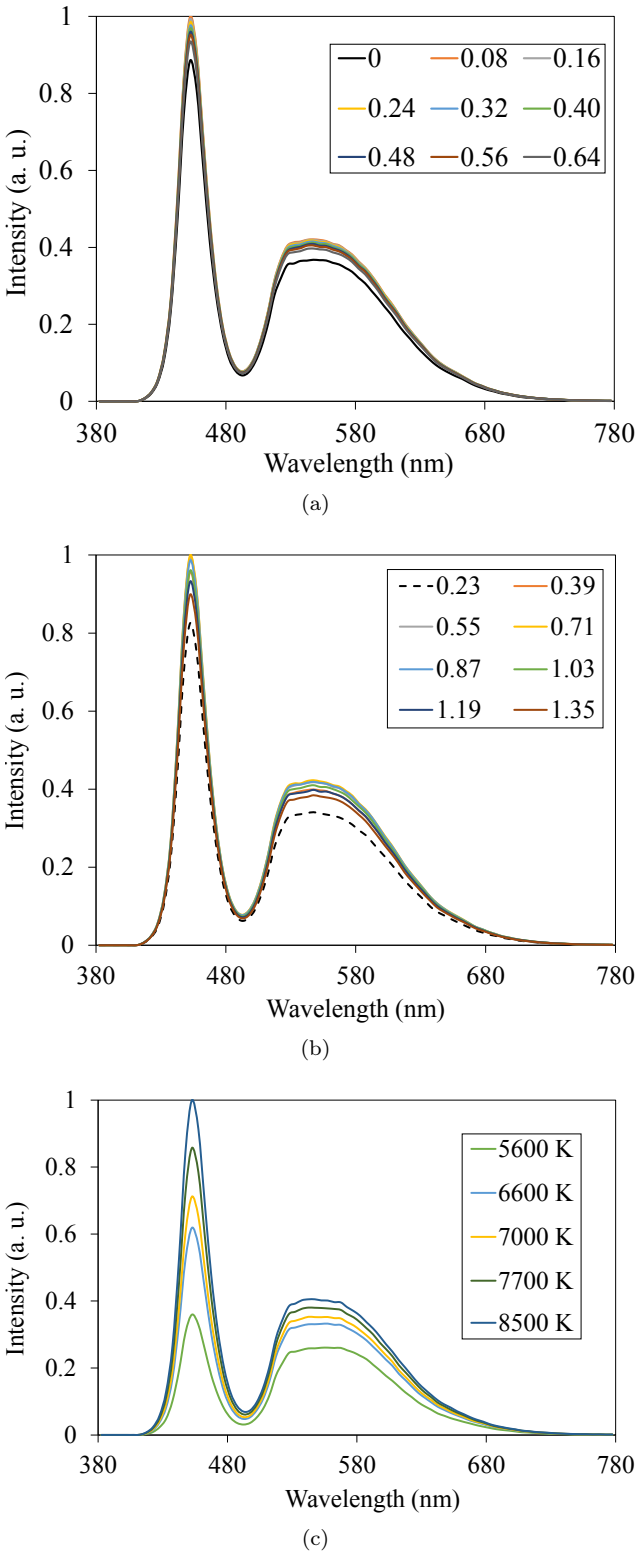


**Fig. 3:** Emission spectra of dual-layer phosphors: (a) case of $d_1$, (b) case of $d_2$ and (c) case of $r_2$.

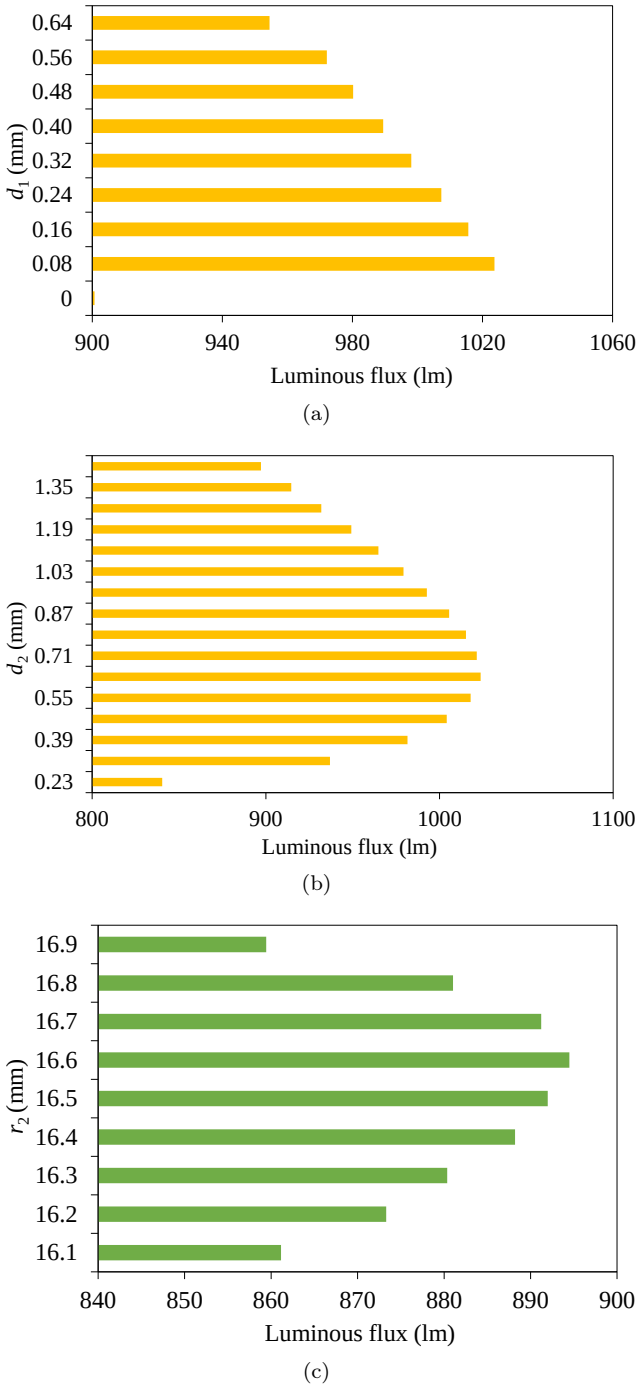


**Fig. 4:** The luminous output of WLEDs at the same CCT in cases of $d_1$ (a), $d_2$ (b) and $r_2$ (c).

## 3. Results and Discussion

In the remote phosphor structure, the lumen efficiency is considerably affected by the distance between the phosphor films and the LED chip surface, owing to the impact of the light loss caused by the scattering, absorption and reflection happening in these gaps, as described in Fig. 4.

In addition, if those distances vary, the light extraction will be affected. Specifically, if the distances $d_1$ and $r_2$ reach the maximum values, which means the underlying phosphor is closest to the LED chip, there will be more lights trapped and reflected in that gap,

and this leads to the thermal increase at the junction, resulting in the decline of the lumen output. However, when these distances, $d_1$, $d_2$, $r_1$, and $r_2$, are adjusted to the appropriate numbers, they will benefit the luminous flux. An enormous change from the beginning is that the lumen output tends to enhance strongly and reach its peak in the range of 0–0.08 mm for $d_1$ and 0.23–0.63 mm for $d_2$.

For FDRP configuration, the luminous flux is maximum at 1020 lm when $d_1 = 0.08$ mm or $d_2 = 0.63$ mm. As for CDRP configuration, the luminous flux gets the highest value at 894 lm when $r_1 = 16$ mm and $r_2 = 16.6$ mm. Conversely, the lumen output has a slight downward trend when the two phosphor layers continuously increase the gap between them, due to the temperature increase at the junction between the phosphor film and the LED chips. This phenomenon can be demonstrated as the following. When the blue light emitted from the blue LED chip, it will reach the lower phosphor layer first and then be converted into yellow light. Still, the light loss inside the LEDs occurs to a portion of the light because of the backscattering, absorption, and reflection whilst the other portion is transmitted through the second phosphor layer after being converted to yellow light. Increasing the distance between two phosphor films causes the lower phosphor layer to move closer to the surface of the LED chips, leading to the increase in the trapped and reflected lights inside the distance between the lower phosphor layer and the LED chips, which also causes the thermal increase at their interface.

In the case of the CDRP structure, the concave surface has an advantage at backscatter light on the surface of the LED chip. Therefore, the energy loss of light emitted is quite a lot. It can be explained that the more $r_2$ increases, the lower the luminous output becomes. When $r_2$ increases up to 16.9 mm, the phosphor surface will be near the LED chip surface, and light will backscatter most at that time. Except for the after scattering phenomenon on the LED surface of the underlying phosphor layer, there is the same phenomenon to the upper phosphor layer in the condition of the CDRP structure. As $r_2$ increases from 16.1 mm to 16.6 mm, the scattering energy decreases as the distance between the two phosphor layers increases. It creates an opportunity for light rays to direct the progress, which makes the luminous flux increase. Otherwise, when $r_2$ increases, the distance between the phosphor layer and the phosphor surface is closer. As a result, the posterior scattering of this lower phosphor layer increases, resulting in the reduced luminous flux. The output luminous flux depends on the different phosphor coatings of the two FDRP and CDRP structures. Compared to the CDRP structure, lights are able to pass straight through the two phosphor layers more easily with the FDRP structure.

# 4. Conclusions

In conclusion, this research analyzed and demonstrated specifically the effects of the distance between the two phosphor layers as well as the gap between the phosphor layer and the LED surface on the optical characteristics of the dual-layer remote phosphor package. The results showed that different phosphor coatings of FDRP and CDRP structures would highly affect the output luminous flux. Therefore, in the FDRP structure, lights can pass straight through the two phosphor layers more easily than in the CDRP structure. The analyzed results also exhibited a significant improvement in lumen output when the phosphor layers are placed in appropriate positions in WLED packages. The luminous flux remarkably rises and reaches the maximum value when $d_1 = 0.08$ mm or $d_2 = 0.63$ mm, while the color uniformity value reduces in both cases. Meanwhile, if $d_1$ is larger than 0.08 mm or $d_2$ is bigger than 0.63 mm, the lumen efficiency and the color deviation have a slump trend. This is because the lights trapped, absorbed, and re-scattered inside the WLED packages increase. Besides that, the chemical transformation of the heated phosphor layer also contributes to that reduction. Hence, studying an appropriate distance between phosphor layers in the dual-layer remote phosphor structure becomes one of the most crucial factors in fabricating high-quality WLEDs.

# References

[1] TANG, Y., L. ZHI, G. LIANG, Z. LI, J. LI and B. YU. Enhancement of luminous efficacy for LED lamps by introducing polyacrylonitrile electrospinning nanofiber film. *Optics Express*. 2018, vol. 26, iss. 21, pp. 27716–27725. ISSN 1094-4087. DOI: 10.1364/OE.26.027716.

[2] FOND, B., C. ABRAM, M. POUGIN and F. BEYRAU. Investigation of the tin-doped phosphor $(Sr,Mg)_3(PO_4)_2$:$Sn^{2+}$ for fluid temperature measurements. *Optical Materials Express*. 2019, vol. 9, iss. 2, pp. 802–818. ISSN 2159-3930. DOI: 10.1364/OME.9.000802.

[3] YUCE, H., T. GUNER, S. BALCI and M. M. DEMIR. Phosphor-based white LED by various glassy particles: control over luminous efficiency. *Optics Letters*. 2019, vol. 44, iss. 3, pp. 479–482. ISSN 1539-4794. DOI: 10.1364/OL.44.000479.

[4] YUAN, Y., D. WANG, B. ZHOU, S. FENG, M. SUN, S. ZHANG, W. GAO, Y. BI and H. QIN. High luminous fluorescence generation using Ce:YAG transparent ceramic excited by

blue laser diode. *Optical Materials Express*. 2018, vol. 8, iss. 9, pp. 2760–2767. ISSN 2159-3930. DOI: 10.1364/OME.8.002760.

[5] CHUNG, S.-R., C.-B. SIAO and K.-W. WANG. Full color display fabricated by CdSe bi-color quantum dots-based white light-emitting diodes. *Optical Materials Express*. 2018, vol. 8, iss. 9, pp. 2677–2686. ISSN 2159-3930. DOI: 10.1364/OME.8.002677.

[6] STEUDEL, F., T. LISEC, P. W. NOLTE, U. HOFMANN, T. VON WANTOCH, F. LOFINK and S. SCHWEIZER. Pixelated phosphors for high-resolution and high-contrast white light sources. *Optics Express*. 2018, vol. 26, iss. 20, pp. 26134–26144. ISSN 1094-4087. DOI: 10.1364/OE.26.026134.

[7] TANG, L., H. YE and D. XIAO. Photo-induced luminescence degradation in Ce, Yb co-doped yttrium aluminum garnet phosphors. *Applied Optics*. 2018, vol. 57, iss. 26, pp. 7627–7633. ISSN 2155-3165. DOI: 10.1364/AO.57.007627.

[8] LEI, R., D. DENG, X. LIU, F. HUANG, H. WANG, S. ZHAO and S. XU. Influence of excitation power and doping concentration on the upconversion emission and optical temperature sensing behavior of $Er^{3+}$: $BaGd_2(MoO_4)_4$ phosphors. *Optical Materials Express*. 2018, vol. 8, iss. 10, pp. 3023–3035. ISSN 2159-3930. DOI: 10.1364/OME.8.003023.

[9] HUANG, X., J. LIANG, B. LI, L. SUN and J. LIN. High-efficiency and thermally stable far-red-emitting $NaLaMgWO_6$:$Mn^{4+}$ phosphors-for indoor plant growth light-emitting diodes. *Optics Letters*. 2018, vol. 43, iss. 14, pp. 3305–3308. ISSN 1539-4794. DOI: OL.43.003305.

[10] BAKHMET'EV, V. V., M. M. SYCHEV, K. A. OGURTSOV, A. S. KOZLOV, A. A. KOTOMIN and S. A. DUSHENOK. Effect of copper introduction and shock-wave processing of zinc sulfide on the spectral characteristics of a manganese-activated phosphor synthesized from it. *Journal of Optical Technology*. 2018, vol. 85, iss. 6, pp. 367–370. ISSN 1091-0786. DOI: 10.1364/JOT.85.000367.

[11] MA, Y., M. WANG, J. SUN, R. HU and X. LUO. Phosphor modeling based on fluorescent radiative transfer equation. *Optics Express*. 2018, vol. 26, iss. 13, pp. 16442–16455. ISSN 1094-4087. DOI: 10.1364/OE.26.016442.

[12] WEN, Z., C. MA, C. ZHAO, F. TANG, Z. CAO, Z. CAO, X. YUAN and Y. CAO. Fabrication and optical properties of $Pr^{3+}$-doped Ba (Sn, Zr, Mg, Ta) $O_3$ transparent ceramic phosphor. *Optics Letters*. 2018, vol. 43, iss. 11, pp. 2438–2441. ISSN 1539-4794. DOI: 10.1364/OL.43.002438.

[13] SONG, X., Z. LIU, Y. XIANG and K. AYDIN. Biaxial hyperbolic metamaterials using anisotropic few-layer black phosphorus. *Optics Express*. 2018, vol. 26, iss. 5, pp. 5469–5477. ISSN 1094-4087. DOI: 10.1364/OE.26.005469.

[14] CAO, J., J. ZHANG and X. LI. Upconversion luminescence of $Ba_3La(PO_4)_3$:$Yb^{3+}$-$Er^{3+}$/$Tm^{3+}$ phosphors for optimal temperature sensing. *Applied Optics*. 2018, vol. 57, iss. 6, pp. 1345–1350. ISSN 2155-3165. DOI: 10.1364/AO.57.001345.

[15] PENG, Y., Y. MOU, X. GOU, X. XU, H. LI, M. CHEN and X. LUO. Flexible fabrication of a patterned red phosphor layer on a YAG:$Ce^{3+}$ phosphor-in-glass for high-power WLEDs. *Optical Materials Express*. 2018, vol. 8, iss. 3, pp. 605–614. ISSN 2159-3930. DOI: 10.1364/OME.8.000605.

[16] LEE, H., S. KIM, J. HEO and W. J. CHUNG. Phosphor-in-glass with Nd-doped glass for a white LED with a wide color gamut. *Optics Letters*. 2018, vol. 43, iss. 4, pp. 627–630. ISSN 1539-4794. DOI: 10.1364/OL.43.000627.

[17] YU, H.-Y., G.-Y. CAO, J.-H. ZHANG, Y. YANG, W.-L. SUN, L.-P. WANG and N.-Y. ZOU. Solar spectrum matching with white OLED and monochromatic LEDs. *Applied Optics*. 2018, vol. 57, iss. 10, pp. 2659–2666. ISSN 2155-3165. DOI: 10.1364/AO.57.002659.

[18] JIANG, P., Y. PENG, Y. MOU, H. CHENG, M. CHEN and S. LIU. Thermally stable multi-color phosphor-in-glass bonded on flip-chip UV-LEDs for chromaticity-tunable WLEDs. *Applied Optics*. 2017, vol. 56, iss. 28, pp. 7921–7926. ISSN 2155-3165. DOI: 10.1364/AO.56.007921.

[19] DINAKARAN, D., C. GOSSLER, C. MOUNIR, O. PAUL, U. T. SCHWARZ and P. RUTHER. Phosphor-based light conversion for miniaturized optical tools. *Applied Optics*. 2017, vol. 56, iss. 13, pp. 3654–3659. ISSN 2155-3165. DOI: 10.1364/AO.56.003654.

[20] WANG, Z., S. LOU, P. LI and Z. LIAN. Single-phase tunable white-light-emitting $Sr_3La(PO_4)_3$:$Eu^{2+}$,$Mn^{2+}$ phosphor for white LEDs. *Applied Optics*. 2017, vol. 56, iss. 4, pp. 1167–1172. ISSN 2155-3165. DOI: 10.1364/AO.56.001167.

[21] XU, M., H. ZHANG, Q. ZHOU and H. WANG. Effects of spectral parameters on the light properties of red-green-blue white light-emitting diodes. *Applied Optics*. 2016, vol. 55, iss. 16, pp. 4456–4460. ISSN 2155-3165. DOI: 10.1364/AO.55.004456.

# About Authors

**Phung Ton THAT** was born in Thua Thien-Hue, Vietnam. He received the B.Sc. degree in electronics and telecommunications engineering (2007) and the M.Sc. degree in electronics engineering (2010) from the University of Technology, Vietnam. He is currently a lecturer at the Faculty of Electronics Technology (FET), Industrial University of Ho Chi Minh City. His research interests are optical materials, wireless communication in 5G, energy harvesting, performance of cognitive radio, physical layer security and NOMA.

**Nguyen Thi Phuong LOAN** was born in Da Nang province, Vietnam. In 2006, she received her master degree from University of Natural Sciences. Her research interest is optoelectronics. She has worked at the Faculty of Fundamental 2, Posts and Telecommunications Institute of Technology, Ho Chi Minh City, Vietnam.

**Nguyen Doan Quoc ANH** was born in Khanh Hoa province, Vietnam. In 2014, Anh received his Ph.D. degree from National Kaohsiung University of Applied Sciences, Taiwan. His research interest is optoelectronics. He has worked at the Faculty of Electrical and Electronics Engineering, Ton Duc Thang University.

**Anh-Tuan LE** (corresponding author) received his B.Sc. in Mechatronics Engineering from University of Technical Education and M.Sc. in Automation Engineering from University of Technology, Hochiminh City, Vietnam in 2006 and 2010, respectively, and Ph.D. in Mechanical and Automatic Engineering from Da-Yeh University, Taiwan, in 2016. He is currently working as a lecturer in Faculty of Electrical and Electronic Engineering, Ton Duc Thang University, Ho Chi Minh City, Vietnam. His current research interests are process control and automation, optics, robot dynamics, vehicle dynamics, vehicle stability control, antilock braking system, traction control system and control applications for vehicles and three-wheeled mobile robots.